

# Insight into the Complexation of Actinides and Lanthanides with Diglycolamide Derivatives: Experimental and Density Functional Theoretical Studies

Arijit Sengupta,<sup>†</sup> Arunasis Bhattacharyya,<sup>†</sup> Willem Verboom,<sup>‡</sup> Sk. Musharaf Ali,<sup>§</sup> and Prasanta K. Mohapatra<sup>\*,†</sup>

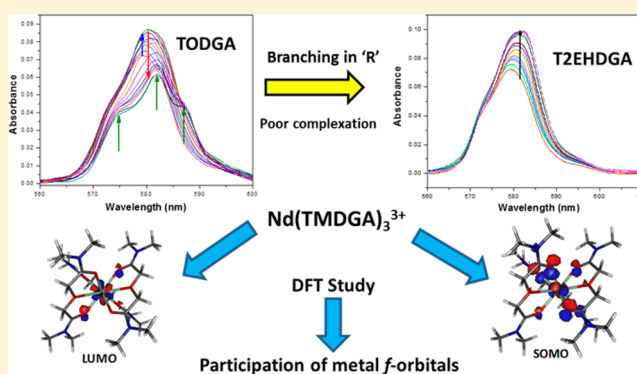
<sup>†</sup>Radiochemistry Division, Bhabha Atomic Research Centre, Trombay, Mumbai 400085, India

<sup>‡</sup>Laboratory of Molecular Nanofabrication, MESA+ Institute for Nanotechnology, University of Twente, P.O. Box 217, 7500 AE Enschede, The Netherlands

<sup>§</sup>Chemical Engineering Division, Bhabha Atomic Research Centre, Trombay, Mumbai 400085, India

## Supporting Information

**ABSTRACT:** Extraction of actinide ( $\text{Pu}^{4+}$ ,  $\text{UO}_2^{2+}$ ,  $\text{Am}^{3+}$ ) and lanthanide ( $\text{Eu}^{3+}$ ) ions was carried out using different diglycolamide (DGA) ligands with systematic increase in the alkyl chain length from *n*-pentyl to *n*-dodecyl. The results show a monotonous reduction in the metal ion extraction efficiency with increasing alkyl chain length and this reduction becomes even more prominent in case of the branched alkyl (2-ethylhexyl) substituted DGA (T2EHDGA) for all the metal ions studied. Steric hindrance provided by the alkyl groups has a strong influence in controlling the extraction behavior of the DGAs. The distribution ratio reduction factor, defined as the ratio of the distribution ratio values of different DGAs to that of T2EHDGA, in *n*-dodecane follows the order  $\text{UO}_2^{2+} > \text{Pu}^{4+} > \text{Eu}^{3+} > \text{Am}^{3+}$ . Complexation of  $\text{Nd}^{3+}$  was carried out with the DGAs in methanol by carrying out UV–vis spectrophotometric titrations. The results indicate a significant enhancement in the complexation constants upon going from methyl to *n*-pentyl substituted DGAs. They decreased significantly for DGAs containing alkyl substituents beyond the *n*-pentyl group, which corresponds to the observed trend from the solvent extraction studies. DFT-based calculations were performed on the free and the  $\text{Nd}^{3+}$  complexes of the DGAs both in the gas and the solvent (methanol) phase and the results were compared the experimental observations. Luminescence spectroscopic investigations were carried out to understand the complexation of  $\text{Eu}^{3+}$  with the DGA ligands and to correlate the nature of the alkyl substituents on the photophysical properties of the  $\text{Eu}(\text{III})$ -DGA complexes. The monoexponential nature of the decay profiles of the complex revealed the predominant presence of single species, while no water molecules were present in the inner coordination sphere of the  $\text{Eu}^{3+}$  ion.



## INTRODUCTION

Trivalent actinides (e.g.,  $\text{Am}^{3+}$ ,  $\text{Cm}^{3+}$ ) are poorly extracted in the tri-*n*-butyl phosphate (TBP)-based plutonium uranium reduction extraction (PUREX) process due to their lower ionic potential as compared to the favorably extracted actinide ions, such as  $\text{UO}_2^{2+}$  and  $\text{Pu}^{4+}$ . The trivalent actinides are, therefore, partitioned into the aqueous raffinate stream which is subsequently concentrated and known as high level nuclear waste (HLW). The major sources of radioactivity and radiation dose in HLW are due to the presence of a number of fission products, viz.  $^{137}\text{Cs}$  and  $^{90}\text{Sr}$  in significant amounts, which will ultimately decay into stable nuclides in a few hundred years. The minor actinides (includes the trivalent actinides, such as Am and Cm and several long-lived Np isotopes) present in the HLW, on the other hand, will survive until several millions of years. The requirement for long-term surveillance of the

vitrified HLW can be avoided if the minor actinides are separated from the HLW and can be managed in a more efficient manner because of their presence in much smaller quantities. A number of ligands, viz. trialkyl phosphine oxide (TRPO), carbamoyl methylene phosphine oxide (CMPO), and diamides including the malonamides, have been investigated extensively for the partitioning of minor actinides from HLW.<sup>1–3</sup> All the processes developed based on the above-mentioned extractants, however, have their own limitations. Sasaki and Choppin<sup>4</sup> introduced a new class of tridentate ligand, the diglycolamides (DGAs; Figure 1), for minor actinide partitioning. A number of literature reports are available on the

Received: November 8, 2016

Revised: February 16, 2017

Published: March 3, 2017

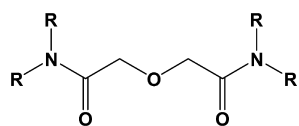


Figure 1. Structural formula of diglycolamide derivatives.

extraction studies of actinides and lanthanides employing DGA-based ligands, such as TODGA (*N,N,N',N'*-tetra-*n*-octyldiglycolamide), and over the years it was found to be one of the most promising extractants for this purpose.<sup>5–7</sup> Brown et al.<sup>8</sup> studied the loading of Th<sup>4+</sup> and Pu<sup>4+</sup> in a TODGA-based extraction system varying the phase modifier and found 0.2 M TODGA and 0.5 M dimethyl dioctyl hexyl-ethoxy malonamide (DMDOHEMA) in kerosene as the optimum formulation from the extraction as well as stripping point of view.

A number of interesting phenomena in the comparative extraction behavior of actinides in different oxidation states employing DGA derivatives is not yet well understood. It is of interest to study the complexation behavior of these DGA derivatives in order to further understand their extraction behavior. A number of literature reports are available, where the lanthanide/actinide complexation has been studied with various DGA derivatives.<sup>9–16</sup> In most of the literature reports, however, the effect of the alkyl substituent was studied using solvent extraction-based technique. Wilden et al.<sup>17</sup> have performed time-resolved laser-induced fluorescence spectroscopic (TRLFS) studies to understand the complexation of Cm<sup>3+</sup> and Eu<sup>3+</sup> in order to understand their extraction behavior, where the selectivity (Eu/Am) obtained from the solvent extraction studies was nicely corroborated with the selectivity (Eu/Cm) obtained from the TRLFS study. In all their ligands, however, the *N*-alkyl group was not altered and only methyl group was successively attached to the etheric carbon of the DGA. Zhu et al., reported a size selective complexation behavior of TODGA-based aggregates for metal ions with ionic radii of ca. 100 pm.<sup>18</sup> It is known that the extraction of the uranyl ion is much lower than that of the tri/tetravalent actinide ions and the nature of the extracted species is influenced by the aqueous feed nitric acid concentration.<sup>19</sup> All these results indicate that the complexation/structures of the actinide–DGA complexes are not yet clearly understood.

Tian et al.<sup>16</sup> have thoroughly studied the Nd<sup>3+</sup> complexation with the tetramethyl derivative of DGA (TMDGA) and the corresponding carboxylic acids, viz. *N,N*-dimethyl-3-oxa-glutaric acid (DMOGA), and oxidiacetic acid (ODA) in the aqueous and solid phases with the help of UV–vis spectrophotometric and single crystal XRD techniques. The UV–vis spectrophotometric studies indicated identical patterns in the hypersensitive absorption band of the Nd<sup>3+</sup> ion during the titration suggesting a similar coordination environment around the Nd<sup>3+</sup> ion. This observation was also validated from the X-ray crystal structure of Nd<sup>3+</sup> complexes of all the three ligands they studied, indicating the formation of a nine-coordinated Nd<sup>3+</sup> ion in a tricapped trigonal prism geometry. In another report by the same group,<sup>20</sup> the complexation of Am<sup>3+</sup> was studied by these techniques. They observed the presence of 1:1, 1:2, and 1:3 complexes in the solution phase by UV–vis spectrophotometric studies. They have also shown similar absorption spectra of the 1:3 complex of Am<sup>3+</sup> in the solution and the solid states. This was due to the complete masking of the Am<sup>3+</sup> ion by three DGA ligands, which resulted in the

similar coordination environment around the Am<sup>3+</sup> ion in both phases.<sup>20</sup>

In the present work, two-phase extraction of lanthanide (Eu<sup>3+</sup>) and actinides in different oxidation states (Am<sup>3+</sup>, Pu<sup>4+</sup>, UO<sub>2</sub><sup>2+</sup>) was studied with different DGAs with varying *N*-alkyl groups (Figure 1: R = *n*-pentyl (TPDGA), *n*-hexyl (THDGA), *n*-octyl (TODGA), *n*-dodecyl (TDDGA), 2-ethylhexyl (T2EHDGA)). UV–vis spectrophotometric titrations were also carried out in order to study the single phase complexation of Nd<sup>3+</sup> with different DGA derivatives (Figure 1: R = methyl (TMDGA), *n*-pentyl, *n*-hexyl, *n*-octyl, *n*-dodecyl, 2-ethylhexyl). Finally, DFT studies were performed on the Nd<sup>3+</sup> complexes of the DGA ligands to explain the experimental observation of their relative complexation/extraction strength.

## EXPERIMENTAL SECTION

**Materials.** The DGA ligands, obtained from Thermax Ltd., Pune, India, as gift samples, were used after checking their purities by <sup>1</sup>H NMR, HR-MS, and HPLC. *n*-Dodecane (Lancaster, UK) was used as procured. Suprapur nitric acid (Merck, Germany) was used for preparing the dilute acid solutions, which was done with Milli-Q (Millipore, USA) water. All the other reagents were of AR grade. <sup>241</sup>Am, <sup>239</sup>Pu, and <sup>235</sup>U tracers were used from laboratory stock solutions, while <sup>152,154</sup>Eu was procured from BRIT (Board of Radiation and Isotope Technology), Mumbai. All the radiotracers were used after checking their radiochemical purities by alpha/gamma ray spectrometry. The gamma ray emitting radionuclides were assayed by a NaI(Tl) scintillator counter (Para Electronics) coupled to a multichannel analyzer (ECIL, India), while the alpha emitting radionuclides were assayed by a liquid scintillator counting system (Hidex, Finland) using toluene-based scintillator cocktails to avoid quenching.

**Solvent Extraction Studies.** Equal volumes (usually 1 mL) of the aqueous phase, containing the radiotracer of interest in 3 M HNO<sub>3</sub> and the organic phase containing 0.1 M DGAs in *n*-dodecane were equilibrated in Pyrex glass tubes for half an hour (which ensured attainment of equilibrium) in a thermostated water bath at 25 ± 0.1 °C. Subsequently, the tubes were centrifuged for 2 min followed by radiometric assay of suitable aliquots (usually, 100 μL) removed from both the phases to calculate the distribution ratio (*D*) value as the ratio of the concentration of the radiotracer (expressed as counts per unit time per unit volume) in the organic phase to that in the aqueous phase.

**Luminescence Spectroscopy.** The organic extracts of the complexes of Eu<sup>3+</sup> with the DGA ligands were prepared by extracting the metal ion quantitatively from 3 M HNO<sub>3</sub> under favorable conditions in *n*-dodecane medium. The composition of the samples for luminescence studies were, therefore, 0.01 M Eu<sup>3+</sup> in 0.1 M DGA derivatives in *n*-dodecane.

**UV–vis Spectroscopy.** Neodymium nitrate hexahydrate (Nd(NO<sub>3</sub>)<sub>3</sub>·6H<sub>2</sub>O) procured from Sigma-Aldrich was used for the complexation studies. A 1.0 × 10<sup>−2</sup> M Nd<sup>3+</sup> solution was titrated against suitable aliquots of DGAs in methanol medium. The overall ionic strength of the medium was maintained at 0.06 using tetramethylammonium nitrate (TMAN). The details of the procedure followed to calculate the conditional stability constant values are provided in the Supporting Information.

**Instrumentation.** Photoluminescence emission and excitation spectra were recorded on an Edinburgh FLS-900 unit augmented with CD-920 controller M 300 dual monochromators in the 200–750 nm region with a Peltier cooled

**Table 1. Distribution Ratios ( $D_M$ ) of Metal Ions Using Different Diglycolamides (DGAs) and the Distribution Ratio Reduction Factors ( $RD_M$ )<sup>a</sup>**

ligand	$D_{Am(III)}$	$D_{Eu(III)}$	$D_{Pu(IV)}$	$D_{U(VI)}$	$RD_{Am}$	$RD_{Eu}$	$RD_{Pu}$	$RD_U$
TPDGA	440	486	152	42	13	21	30	111
THDGA	380	398	127	25	11	17	25	66
TODGA	321	330	109	11	9	14	22	29
TDDGA	225	218	68	3	6	9	14	8
T2EHDGA	35	23	5	0.38	1	1	1	1

<sup>a</sup>Org. phase: 0.1 M DGA in *n*-dodecane; aq. phase: 3 M HNO<sub>3</sub> containing the radiotracer of different metal ions.

photomultiplier tube as detector. A 150 W xenon flash lamp having variable frequency range of 10 to 100 Hz was used as the excitation source. Multiple emission and excitation scans (at least five) were taken to minimize the fluctuations in peak intensity and maximize signal–noise ratio. The acquisition and analysis of the data were carried out by F-900 software supplied by Edinburgh Analytical Instruments, UK.

UV–vis spectrophotometric measurements were carried out using a JASCO V530 double beam spectrophotometer using quartz cells as sample holders in the wavelength range of 600–1000 nm with a scan rate of 100 nm/min. <sup>1</sup>H NMR spectra of free DGA derivatives and their lanthanum triflate complexes were recorded in methanol-*d*<sub>4</sub> using a BRUKER 200 MHz NMR spectrometer.

**Computational Studies.** Gas phase geometries of the free DGAs and its Nd<sup>3+</sup> complexes of the type ML<sub>3</sub><sup>3+</sup> were optimized at the GGA level of density functional theory (DFT) by using the B3LYP density functional.<sup>21–23</sup> Twenty eight electron core potentials (ECPs) along with the corresponding def-SV(P) basis set were chosen for Nd<sup>3+</sup>. All the other lighter atoms were treated at the all electron (AE) level. All the calculations were performed using the TURBOMOLE-7.0 program package.<sup>24,25</sup> In order to have a quantitative idea about the comparative “Nd–O” bond strength for the Nd<sup>3+</sup> complexes the molecular orbitals were analyzed to calculate the two center Mayer’s and Weiberg’s bond order using the AOMix program.<sup>26,27</sup>

## RESULTS AND DISCUSSION

**Extraction of Actinides Using Different Diglycolamides.** The distribution ratio ( $D$ ) values of Am<sup>3+</sup>, Eu<sup>3+</sup>, Pu<sup>4+</sup>, and UO<sub>2</sub><sup>2+</sup> have been obtained using TPDGA, THDGA, TODGA, T2EHDGA, and TDDGA. In general, the  $D$  values follow the trend  $D_{Eu} > D_{Am} > D_{Pu} > D_U$  (Table 1). Wei et al.<sup>28</sup> have studied the complexation of trivalent actinide and lanthanide (Am<sup>3+</sup>, La<sup>3+</sup>, Ce<sup>3+</sup>, Nd<sup>3+</sup>) and tetravalent actinide ions (Np<sup>4+</sup>, Pu<sup>4+</sup>) with TMDGA. Significantly smaller stability constant values were found for the tetravalent than for the trivalent ions. The extraordinarily higher extraction efficiency of trivalent actinide and lanthanide ions compared to the tetra- and hexavalent actinide ions was attributed to the formation of suitable reverse micellar aggregation by the DGAs in the *n*-dodecane medium.<sup>29–31</sup> The trivalent lanthanide ions, being hard acids compared to the trivalent actinides, prefer to form stronger complexes with ligands with hard donor atoms.<sup>32,33</sup> The distribution ratio of a particular metal ion followed the trend, TPDGA > THDGA > TODGA > TDDGA > T2EHDGA. This suggested that the extraction efficiency of the DGA derivatives decreased significantly with increasing the chain length of the alkyl groups attached to the amidic “N” atoms. Branching in the alkyl groups further reduced the extraction efficiency of the DGA derivative. Similar observation

was also reported by Sasaki et al.<sup>14</sup> where they have scanned a number of DGA derivatives for the extraction of actinides of different oxidation states, viz. Am(III), Th(IV), Np(V), and U(VI). They showed a nice correlation between the  $D_M$  values with increasing the number of carbon atoms in the alkyl chain attached to the amidic “N” atoms. The deviation was observed only in case of T2EHDGA and *N,N'*-dimethyl-*N,N'*-diphenyl-diglycolamide (DMDPDGA).

A number of factors dictate the extraction capability of the DGA derivatives. As the metal–ligand complexation process is expected to be most probable at the aqueous–organic interface, a high lipophilicity of the DGAs, therefore, does not allow the ligand to come close to the interface and results in poor metal ion complexation and extraction. With increasing alkyl chain from *n*-pentyl (TPDGA) to *n*-dodecyl (TDDGA), the lipophilicity enhances significantly resulting in a poor extraction capability. However, with increasing chain length of the amide substituents, more steric crowding around the ligating sites is expected. Consequently, the approach of the metal ion toward the ligating sites is hindered. This may be another factor responsible for the decrease in the  $D$  values going from TPDGA to TDDGA. Other factor which can also affect the complexation and extraction efficacy of the DGA derivatives is the charge distribution at the coordinating sites due to the change in the alkyl groups. On comparing the extraction efficiency of different DGA ligands toward Am<sup>3+</sup> and Eu<sup>3+</sup>, it was noticed that with increasing the alkyl chain length, the decrease in  $D_{Eu}$  was sharper than that in  $D_{Am}$ . This resulted in lower  $D_{Eu}$  value in case of TDDGA and T2EHDGA as compared to the other ligands. The 2-ethylhexyl substituent, being a secondary alkyl group, further enhanced the steric crowding and consequently, a significantly lower  $D$  value was observed for this ligand. The reduction factor ( $RD_M$  is the ratio of the  $D_M$  values for different diglycolamides to that for T2EHDGA in *n*-dodecane) for the four different metal ions followed the order UO<sub>2</sub><sup>2+</sup> > Pu<sup>4+</sup> > Eu<sup>3+</sup> > Am<sup>3+</sup>. Due to the presence of two axial metal oxo bonds, the approach of the ligands toward the hexavalent actinyl ion (UO<sub>2</sub><sup>2+</sup>) would be only possible through the equatorial side. Therefore, the steric effect is expected to be more pronounced for the uranyl ion resulting in a more than 100 fold reduction in  $D_U$  values obtained with T2EHDGA as compared to those obtained with TPDGA. The ionic radii follow the order Pu<sup>4+</sup> (0.96 Å) < Eu<sup>3+</sup> (1.066 Å) < Am<sup>3+</sup> (1.09 Å).<sup>34</sup> The order of the decrease in the  $D_M$  values for different metal ions with increasing bulkiness of the alkyl groups of the DGAs can, therefore, be nicely explained on the basis of the steric requirements for their coordination.

**UV–vis Spectrophotometric Studies of Nd<sup>3+</sup>Complexation.** In order to understand the extraction behavior of the substituted DGA ligands, the single phase Nd<sup>3+</sup> complexation was studied with various DGAs (TMDGA, TPDGA, THDGA, TODGA, TDDGA, and T2EHDGA) in

methanol medium in the presence of 0.01 M ionic strength (tetramethylammonium nitrate, TMAN) by following the change in the hypersensitive UV–vis absorption band of  $\text{Nd}^{3+}$  at 580 nm with incremental addition of DGA ligands. The change in the absorption spectra of  $\text{Nd}^{3+}$  during the titration with different DGA derivatives (TMDGA, TPDGA, THDGA, TODGA, and T2EHDGA) and the molar absorptivity values for different  $\text{Nd}^{3+}$  complexes obtained by fitting the titration data are shown in the Supporting Information (Figures S1–S5).  $\text{Ho}^{3+}$  complexation of TMDGA has been reported in the aqueous phase in the presence of perchlorate as the counteranion. The solvent extraction data have little relevance for the radioactive waste processing.<sup>9–15</sup> Recently, the same authors have reported the complexation of lanthanide ions, such as  $\text{Sm}^{3+}$ ,  $\text{Eu}^{3+}$ , and  $\text{Tb}^{3+}$ , with TMDGA using a fluorescence-based technique and their results showed a monotonous increase in the complexation constant values with decreasing size of the lanthanide ions.<sup>25</sup>  $\text{Nd}^{3+}$  complexation of TMDGA in aqueous medium in the presence of nitrate as the counteranion is also known.<sup>16</sup> In all these cases, however, the complexation was performed only with TMDGA. Charbonnel et al.<sup>36</sup> have studied the complexation of some lanthanides ( $\text{La}^{3+}$ ,  $\text{Pr}^{3+}$ , and  $\text{Tb}^{3+}$ ) and  $\text{Am}^{3+}$  with the ethyl derivative of DGA (TEDGA), while Pathak et al.<sup>37</sup> have investigated the  $\text{Eu}^{3+}$  complexation with TODGA in acetonitrile using fluorescence spectroscopy. To the best of our knowledge, a systematic study to the single phase complexation of  $\text{Ln}^{3+}$  ions with DGAs with varying size of the alkyl groups is not reported. That would be very interesting, since the solvent extraction experiments showed a significant dependence of the alkyl chains on the extraction behavior of DGA derivatives.

We studied the  $\text{Nd}^{3+}$  complexation with DGA derivatives with a systematic variation of the alkyl groups from methyl to *n*-octyl and 2-ethylhexyl in the presence of nitrate ions; the results are listed in Table 2. Because of the lower aqueous solubility of

**Table 2. Complexation Constants for  $\text{Nd}^{3+}$  with Different Diglycolamides Obtained by UV–Vis Spectrophotometric Titrations in Methanol at Constant Ionic Strength of 0.06**

ligands	$\log \beta_1$	$\log \beta_2$	$\log \beta_3$
TMDGA	3.46	6.66	9.4
TPDGA		9.59	12.92
THDGA		8.17	11.53
TODGA		7.78	10.32
T2EHDGA		7.04	

the DGA derivatives having longer alkyl chains, all complexation studies were carried out in methanol. The results indicated that TMDGA formed all the possible stoichiometries, viz. 1:1, 1:2, and 1:3 complexes of  $\text{Nd}^{3+}$  with  $\log \beta$  values much higher than those reported in case of  $\text{Ho}^{3+}$  complexation.<sup>9</sup> This may be due to the medium effect:  $\text{Nd}^{3+}$  complexation in methanol versus  $\text{Ho}^{3+}$  complexation in aqueous medium.<sup>9</sup> In the case of TPDGA, THDGA, and TODGA only 1:2 and 1:3 complexes were observed and no trace of 1:1 complexes was noticed. In the case of TDDGA, on the other hand, the presence of a 1:1 complex was also observed. It is interesting to note that the  $\log \beta$  values for both the 1:2 and 1:3 complexes increased significantly going from TMDGA to TPDGA, which can easily be explained based on two factors, viz. the higher electron donation ability of the *n*-pentyl group in TPDGA as compared to the methyl group in TMDGA as indicated from

the higher electron density on the coordinating carbonyl and etheral oxygen atoms in TPDGA ( $-0.619$  e and  $-0.580$  e, respectively) as compared to that in TMDGA ( $-0.548$  e and  $-0.545$  e, respectively) calculated using DFT study and the requirement of a higher desolvation energy for TMDGA than for the bulkier TPDGA prior to the complexation with the  $\text{Nd}^{3+}$  ion. Similar increase in the complexation strength of DGA derivatives from TMDGA to *N,N,N',N'*-tetraethyl diglycolamide (TEDGA) and from TEDGA to *N,N,N',N'*-tetra-*n*-propyl diglycolamide (TPrDGA) was also noticed by Sasaki et al.,<sup>13</sup> where they reported maximum decrease in the metal ion extraction in a TODGA-based extraction system using TPrDGA as the aqueous complexant in 1 M  $\text{HNO}_3$  medium. The same group, however, reported maximum reduction in extraction efficiency of TODGA using TEDGA as the aqueous complexing agent in 0.24 M  $\text{HNO}_3$ .<sup>14,15</sup> This could be due to the less aqueous solubility of TPrDGA at lower  $\text{HNO}_3$  concentration, which resulted in lowering in TPrDGA concentration in the aqueous phase leading to insufficient masking of the metal ions in the aqueous phase and higher extraction into the organic phase. Upon further increase of the alkyl chain length, the  $\text{Nd}^{3+}$  complexation ability decreased as reflected in the  $\log \beta$  values, which is clearly the effect of increasing steric requirements with the increasing size of the alkyl groups to accommodate two or three bulky DGA ligands surrounding the metal ion. Steric factors became further prominent in the case of the branched homologue, T2EHDGA, leading to the formation of only 1:2 complex, while the 1:3 complex was not detected. A similar trend was also observed in the solvent extraction studies. This demonstrates that the single phase complexation studies nicely explain the observation from the two-phase solvent extraction studies (*vide supra*).

**Conformational Studies of Uncomplexed Diglycolamides.** DFT-based calculations on the complexation of  $\text{Ln}^{3+}$  and  $\text{An}^{3+}$  with DGAs are well-known in literature.<sup>38–41</sup> In these studies, randomly different DGAs have been used, however, a systematic variation of the alkyl groups has not been taken into account. In the present work, the energies were computed for the different conformations of DGA derivatives (Figure 2 for TMDGA) varying the alkyl groups from methyl to *n*-dodecyl (Table 3). The conformations “f” and “g” do not have any significance for the bonding with the metal ion as one of the two carbonyl groups would remain nonbonded. Therefore, the calculations were not performed for these (“f” and “g”) conformations. It is to be noted here that in conformation “a”, all the three coordinating “O” atoms are in a coplanar geometry and appear to be preorganized for coordination to the metal ion. This was, however, not the lowest energy conformation in any of the DGA derivatives. In case of TMDGA to THDGA, the lowest energy conformation was found to be conformation “e”, where the dihedral angle between the etheric “O” and one of the two carbonyl “O” atoms was  $120^\circ$ , whereas the other carbonyl “O” atom was coplanar with the etheric “O” atom. In the experimentally obtained crystal structure of TMDGA, however, one water molecule formed hydrogen bonds with the two carbonyl “O” atoms of a TMDGA molecule, which forcefully brought all the three “O” atoms into a coplanar geometry (conformation “a”).<sup>28</sup> For TODGA and TDDGA derivatives, however, the conformation “d” was the most stable and in case of TDDGA, the conformation “c” became most stable. The difference in energies between all the conformations for a particular DGA derivative was found to be within  $36 \text{ kJ mol}^{-1}$ . Further increase in alkyl chain length, however, did not

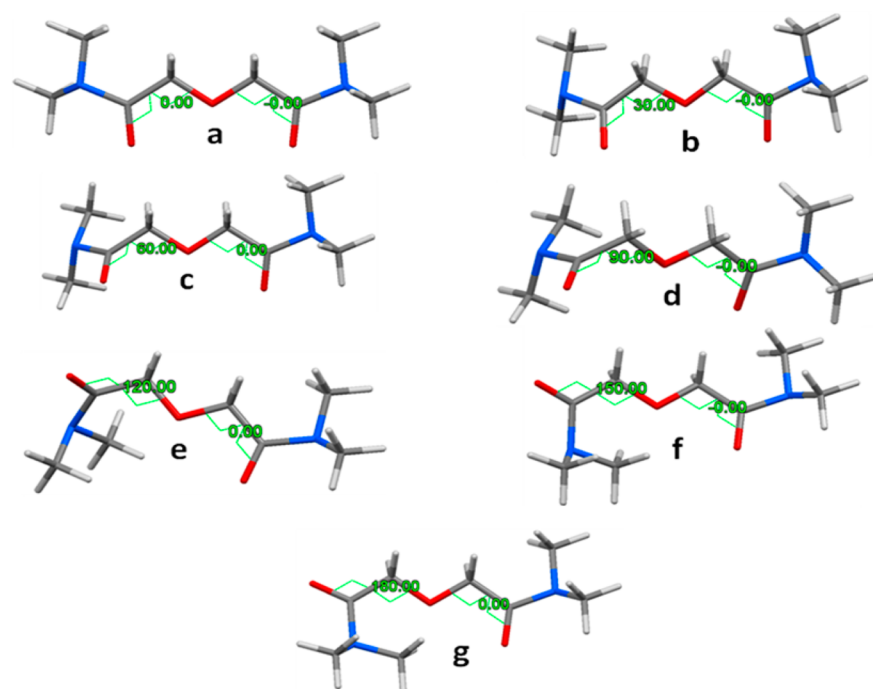


**Figure 2.** Conformations of TMDGA varying the torsional angles between the planes containing the coordinating “O” atoms.

**Table 3. Relative Energies ( $\text{kJ mol}^{-1}$ ) of Various Conformations of  $C_n$ DGAs with Respect to the Lowest Energy Conformation in Figure 2**

DGA	$C_n$	a	b	c	d	e
TMDGA	$C_1$	6.2	16.3	26.4	7.9	0.0
TEDGA	$C_2$	13.1	18.4	8.0	10.0	0.0
TBDGA	$C_4$	14.6	22.7	23.3	11.6	0.0
TPDGA	$C_5$	13.2	26.6	21.6	9.0	0.0
THDGA	$C_6$	21.7	16.0	12.3	3.1	0.0
TODGA	$C_8$	7.3	26.9	31.1	0.0	16.0
TDDGA	$C_{10}$	27.0	29.9	28.6	0.0	8.0
TDDDGA	$C_{12}$	30.1	35.7	0.0	5.6	2.3

increase the steric hindrance significantly, resulting in comparable relative energies of the different conformations of TEDGA to TDDGA.

In order to understand the effect of solvation on the conformational energies of the DGAs, the energies of all the conformations were also calculated in methanol ( $\epsilon = 32.7$ ) and the results are listed in Table 4. For a particular DGA derivative, the solvation energy was found to be the highest in the case of conformation “a”. This is due to the more polar nature of the DGA in this conformation resulting in more

**Table 4. Solvation Energies ( $\text{kJ mol}^{-1}$ ) for Different Conformations of  $C_n$ DGAs in Methanol**

DGA	$C_n$	a	b	c	d	e
TMDGA	$C_1$	-73.2	-69.1	-62.5	-58.3	-53.6
TEDGA	$C_2$	-76.5	-70.3	-63.9	-57.2	-52.5
TBDGA	$C_4$	-75.7	-73.5	-66.4	-60.1	-54.7
TPDGA	$C_5$	-76.9	-75.2	-68.0	-61.8	-55.9
THDGA	$C_6$	-77.0	-76.3	-69.3	-63.1	-57.6
TODGA	$C_8$	-79.2	-77.9	-71.1	-64.9	-58.5
TDDGA	$C_{10}$	-81.4	-79.4	-72.8	-66.8	-60.1
TDDDGA	$C_{12}$	-83.2	-81.1	-74.6	-68.6	-62.3

stabilization in methanol than in the gas phase. Comparing the solvation energies of different DGAs in a particular conformation, it is interesting to note that the solvation energies become more and more negative upon increasing the size of the alkyl chain length.

**Computational Studies on the Neodymium Complexes of Diglycolamides.** The geometries of  $\text{Nd}^{3+}$  complexes of four DGAs (TMDGA, TEDGA, TPrDGA, and TBDGA) were optimized; the geometry-optimized structures of the  $\text{Nd}^{3+}$ -TMDGA complexes are shown in Figure 3. The optimized geometries of all the five  $\text{Nd}^{3+}$  complexes of the different DGA derivatives used for the DFT calculations are shown in Figure S6 and their coordinates are tabulated in Table S1 (Supporting Information). As reported in the literature from the single crystal XRD studies of TMDGA complexes with  $\text{Nd}^{3+}$  and  $\text{Am}^{3+}$ ,<sup>16,20</sup> the nine “O” atoms of three DGA molecules are coordinated in a tricapped trigonal prism geometry around the central  $\text{Nd}^{3+}$  ion, whereas six carbonyl “O” atoms are occupying the six corners of the trigonal prism and the three etheral “O” atoms the three capping positions. The “Nd–O” bond distances for the carbonyl oxygen atoms of TMDGA are comparable to those reported in the X-ray crystal structural analysis of  $\text{NdL}_3(\text{H}_2\text{O})_{7.5}$  (Table 5).<sup>20</sup> The structures obtained from the X-ray crystallography and computational studies showed that “Nd–O” distances varied in a significant range resulting in a deviation of the symmetry of the complexes. The “Nd–O<sub>ether</sub>” bond distances are, however, a little longer in the present calculations than those obtained from the crystal structure. The literature reports based on the quantum chemical calculations also showed that the “M–O<sub>carbonyl</sub>” bond distances are significantly shorter than the “M–O<sub>ether</sub>” bond distances in the cases of various actinide and lanthanide complexes of DGA derivatives studied.<sup>38–42</sup> The “Nd–O” bond distances for the five  $\text{Nd}^{3+}$  complexes of the different DGA derivatives are provided in Table S2 along with those reported in the literature. The results indicate that there is no change in the “Nd–O” bond distances increasing the alkyl chain length

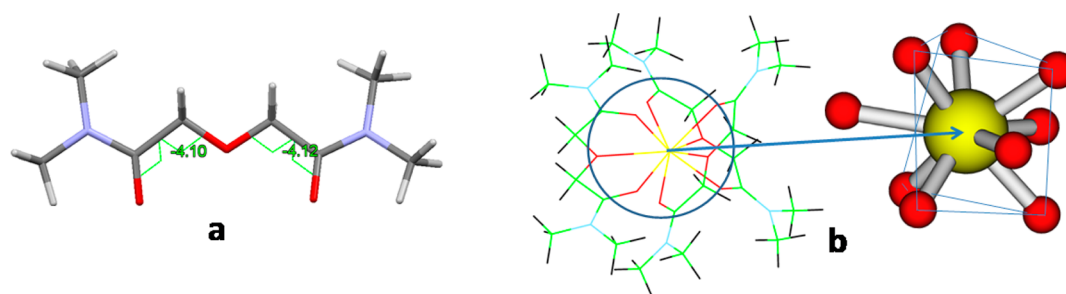


Figure 3. Gas phase geometry optimized structures of (a) TMDGA and (b)  $\text{Nd}(\text{TMDGA})_3^{3+}$  complex.

Table 5. Structural Parameters (“Nd–O” Bond Distances in Å) of the  $\text{Nd}^{3+}$  Complex of TMDGA

complex	p.w.	$\text{NdL}_3(\text{ClO}_4)_3[9]$	$\text{NdL}_3(\text{NO}_3)_3(\text{H}_2\text{O})_2[9]$	$\text{NdL}_3(\text{H}_2\text{O})_{7,5}[9]$
Nd–O <sub>carbonyl</sub>	2.427–2.452	2.402–2.449	2.407–2.439	2.413–2.470
Nd–O <sub>ether</sub>	2.635–2.656	2.526–2.533	2.515–2.549	2.554–2.607

from methyl (TMDGA) to *n*-butyl (TBDGA). Similar observation was also reported in the literature indicating no change in the “M–O” bond distances in the  $\text{Am}^{3+}$  and  $\text{Eu}^{3+}$  complexes of TMDGA and TEDGA.<sup>40,41</sup> The “Nd–O” bond lengths are, however, slightly increasing with branching at the 2-position of the alkyl chain, viz. in case of tetra(2-methylpropyl)diglycolamide (T2MPPrDGA).

It is of interest to rationalize the results of the DFT-based calculations of the  $\text{Nd}^{3+}$  complexation of the different DGAs. The complexation energies ( $\Delta E$ ) for the  $\text{Nd}^{3+}$  complexation with various DGAs (L), following eq 1, have been calculated in the gas phase as well as in methanol medium where the energies for the geometry optimized structures were considered for the free DGA ligands and their respective  $\text{Nd}^{3+}$  complexes (Figure 3).



The  $\Delta E$  values were found to be significantly lower in the solution phase than in the gas phase due to the higher solvation energy of  $\text{Nd}^{3+}$  as compared to that of the complex ( $\text{NdL}_3^{3+}$ ) in a polar solvent like methanol (Table 6). The results indicate

Table 6. Complexation Energies ( $\text{kJ mol}^{-1}$ ) of  $\text{Nd}^{3+}$  with Different DGAs in the Gas Phase and in Methanol According to Eq 1

ligand	$C_n$	gas phase	sol. phase
TMDGA	$C_1$	–3158.3	–888.4
TEDGA	$C_2$	–3208.9	–903.8
TPDGA	$C_3$	–3296.8	–940.7
TBDGA	$C_4$	–3296.2	–916.0
T2MPPrDGA	$C_4$	–3244.6	–870.8

increasing complexation energies with an increase in the size of the alkyl chain length going from TMDGA to TPDGA both in the gas and solution phase. Upon further increase of the alkyl chain length, as with a *n*-butyl group (TBDGA), no increase in the complexation energies was found in the gas phase, while it just decreased in the solution phase. This may be due to the fact that continuous increase of the steric bulk will make the complex more and more unstable. It would be more realistic to compare the complexation strength observed experimentally with Gibb’s free energy ( $\Delta G$ ) values for the complexation with different DGA derivatives.  $\Delta G$  values for the  $\text{Nd}^{3+}$  complex-

ation with different DGA derivatives (eq 1) provided in Table 7 were calculated using the following equation

Table 7. Thermodynamic Parameters (Enthalpies, Entropies, and Gibb’s Free Energies) for the Complexation of  $\text{Nd}^{3+}$  with Different DGAs in the Gas Phase According to Eq 1

ligand	$C_n$	$\Delta H$ ( $\text{kJ mol}^{-1}$ )	$\Delta S$ ( $\text{J mol}^{-1}\cdot\text{K}^{-1}$ )	$\Delta G$ ( $\text{kJ mol}^{-1}$ )
TMDGA	$C_1$	–749.1	–0.1342	–709.124
TEDGA	$C_2$	–761.9	–0.0674	–741.79
TPDGA	$C_3$	–784.6	0.0685	–805.037
TBDGA	$C_4$	–782.3	0.1237	–819.208
T2MPPrDGA	$C_4$	–771.7	0.1139	–805.623

$$\Delta G = \Delta E + \Delta ZPE + \Delta nRT - T\Delta S \quad (2)$$

Here,  $\Delta ZPE$  is the change in zero point energy;  $\Delta n$  is the change in number of molecules;  $R$  is the universal gas constant;  $T$  is the temperature in K; and  $\Delta S$  is the change in entropy for the reaction. It is interesting to note here that with increasing the size of the linear alkyl chain length from methyl (TMDGA) to *n*-butyl (TBDGA), the  $\Delta G$  values for the  $\text{Nd}^{3+}$  complexation became more and more negative, which could result into increasing complexation strength with increasing the linear alkyl chain length. Experimental studies reported in the literature and from the present work also support this theoretical results predicting the order of complexation strength  $\text{TPrDGA} > \text{TEDGA} > \text{TMDGA}$  observed experimentally from the reduction in  $D_M$  values in a TODGA-based extraction system.<sup>13</sup> In case of branched alkyl group (T2MPPrDGA) unfavorable  $\Delta G$  value was observed as compared to the corresponding straight chain alkyl derivative (TBDGA) predicting lower complexation strength of the DGA derivative with branched alkyl group which is also experimentally supported by weaker complexation of T2EHDGA as compared to TODGA from the solvent extraction and UV–vis spectrophotometric studies reported in the present work as well as in the literature.<sup>14</sup>

The frontier orbitals of the  $\text{Nd}^{3+}$  complex of TMDGA were analyzed using natural population analysis (NPA) (Figure 4). Significant contributions of the neodymium “*f*” orbitals were noticed in the high lying molecular orbitals (LUMO, SOMO, SOMO-1), whereas lower lying MOs were found to be mainly ligand-based. In order to understand the effect of branching in the alkyl chain, a DFT calculation was performed on the  $\text{Nd}^{3+}$

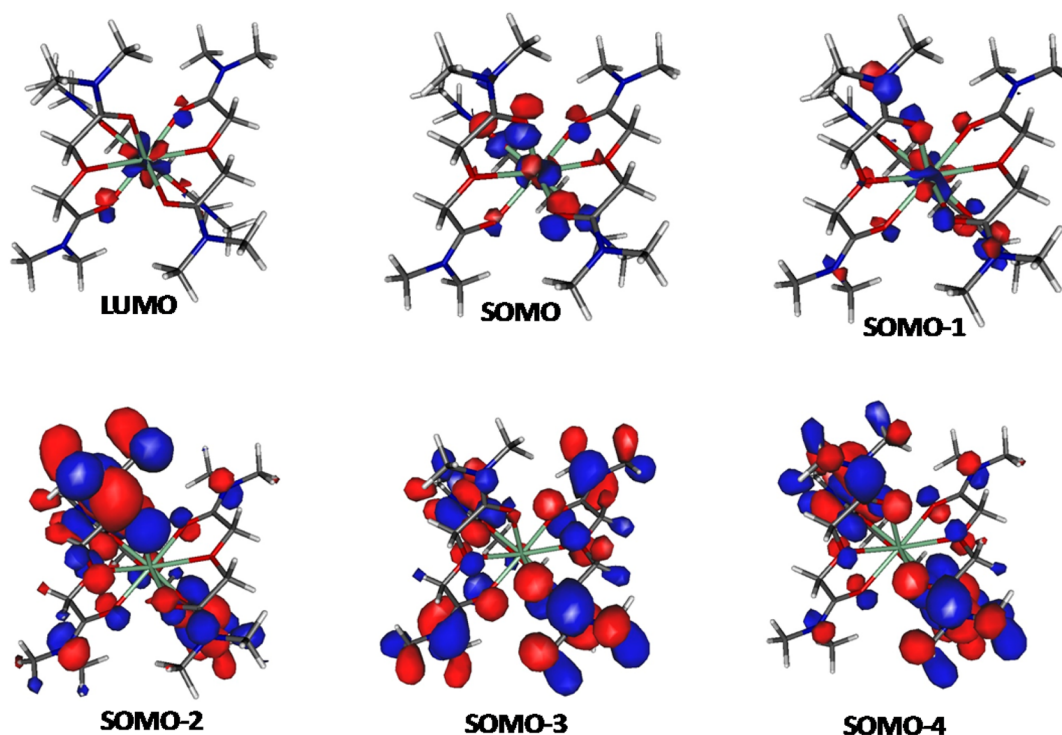


**Figure 4.** Frontier molecular orbitals of the  $\text{Nd}^{3+}$  complex of TMDGA ( $\text{Nd}(\text{TMDGA})_3^{3+}$ ) showing the contribution of the metal “4f” and ligand orbitals.

complex of T2MPrDGA, which can be considered as the lower homologue of T2EHDGA. The results (Table 6) show that the complexation energy for T2MPrDGA is significantly lower as compared to that of its straight chain analogue, i.e., TBDGA. This nicely explains the lower complexation as well as extraction ability of T2EHDGA observed from the UV–vis spectrophotometric and solvent extraction studies.

**Luminescence of Extracted Eu-Diglycolamide Complexes.** Diglycolamide-based ligands are found to extract trivalent lanthanides and actinides from aqueous acidic waste solutions. Though the stoichiometry of the extracted complex and the separation behavior of actinides and lanthanides were studied by the solvent extraction technique,<sup>43</sup> it is important to understand the nature of the extracted species, i.e., whether the complexes are free from inner-sphere water molecules or not, the number of species present during the complexation, the nature of bonding between the metal ions and the ligating atoms, etc. Therefore, time-resolved fluorescence spectroscopy (TRFS) studies were carried out, using  $\text{Eu}^{3+}$  as a surrogate for the trivalent actinide ions in the organic extract consisted of 0.1 M DGA derivatives in *n*-dodecane. The inner-sphere hydration number ( $N_{\text{H}_2\text{O}}$ ) of Ln(III), which provides important information on the coordination behavior of the Ln(III) ions in their complexes, can be obtained by using the difference in the decay constant ( $k_{\text{obs}}$ , the reciprocal of the lifetime of the excited state) in  $\text{H}_2\text{O}$  and  $\text{D}_2\text{O}$  system with following formula<sup>44</sup>

$$N_{\text{H}_2\text{O}} = C(k_{\text{obs}}(\text{H}_2\text{O}) - k_{\text{obs}}(\text{D}_2\text{O})) \quad (3)$$

where  $k_{\text{obs}}(\text{H}_2\text{O})$  and  $k_{\text{obs}}(\text{D}_2\text{O})$  are the decay constant of metal ions in  $\text{H}_2\text{O}$  and  $\text{D}_2\text{O}$  systems, respectively, and  $C$  is a characteristic constant for each Ln(III). Generally,  $k_{\text{obs}}(\text{H}_2\text{O}) \gg k_{\text{obs}}(\text{D}_2\text{O})$  and  $k_{\text{obs}}(\text{D}_2\text{O})$  is almost a constant, and ligands are not as effective as  $\text{H}_2\text{O}$  in causing the de-excitation of the excited state, therefore, the hydration number can be obtained

from the decay constant. For Eu(III) the eq 3 was simplified to eq 4 in order to determine the number of the inner-sphere water molecules<sup>45</sup>

$$N_{\text{H}_2\text{O}} = (1.05 \times 10^{-3}/\tau) - 0.44 \quad (4)$$

where “ $\tau$ ” is the lifetime of the excited species in seconds and  $N_{\text{H}_2\text{O}}$  the number of water molecules. For all the  $\text{EuL}_3^{3+}$  complexes, no water molecules were found to be associated in the inner sphere of the  $\text{Eu}^{3+}$  ion. The decay curves (Figure S7 in the Supporting Information) of all  $\text{Eu}^{3+}$ –complexes follow a monoexponential pattern indicating the predominant presence of single species. Solvent extraction studies showed that three to four DGA ligands are associated with a single trivalent actinide ion in molecular diluents like *n*-dodecane.<sup>7,8</sup> In the present study, an attempt was made to correlate the effect of different alkyl groups at the DGAs on the photophysical properties of the respective  $\text{Eu}^{3+}$  complexes. In the luminescence profiles of all the  $\text{Eu}^{3+}$  complexes (Figure 5), five sets of emission lines were assigned to the particular transition (1st set at  $\sim 580 \text{ nm} - {}^5\text{D}_0 \rightarrow {}^7\text{F}_0$  transition, second set at  $\sim 593 \text{ nm} - {}^5\text{D}_0 \rightarrow {}^7\text{F}_1$  transition, third set at  $\sim 613 \text{ nm} - {}^5\text{D}_0 \rightarrow {}^7\text{F}_2$  transition, fourth set at  $\sim 650 \text{ nm} - {}^5\text{D}_0 \rightarrow {}^7\text{F}_3$  transition, and fifth set at  $\sim 700 \text{ nm} - {}^5\text{D}_0 \rightarrow {}^7\text{F}_4$  transition).<sup>46</sup> The high intensity of the  ${}^5\text{D}_0 \rightarrow {}^7\text{F}_2$  transition reveals that the  $\text{Eu}^{3+}$  ion resides in asymmetric environments with respect to the center of symmetry and it can be quantified as the asymmetry factor ( $A$ ) using the equation below:<sup>44–47</sup>

$$A = I({}^5\text{D}_0 \rightarrow {}^7\text{F}_2)/I({}^5\text{D}_0 \rightarrow {}^7\text{F}_1) \quad (5)$$

where  $I({}^5\text{D}_0 \rightarrow {}^7\text{F}_2)$  and  $I({}^5\text{D}_0 \rightarrow {}^7\text{F}_1)$  refer to the intensities of the  ${}^5\text{D}_0 \rightarrow {}^7\text{F}_2$  and the  ${}^5\text{D}_0 \rightarrow {}^7\text{F}_1$  transitions, respectively.  ${}^5\text{D}_0 \rightarrow {}^7\text{F}_1$  transitions being the magnetic-dipole transitions, the  $I({}^5\text{D}_0 \rightarrow {}^7\text{F}_1)$  values are independent of the ligand field. The

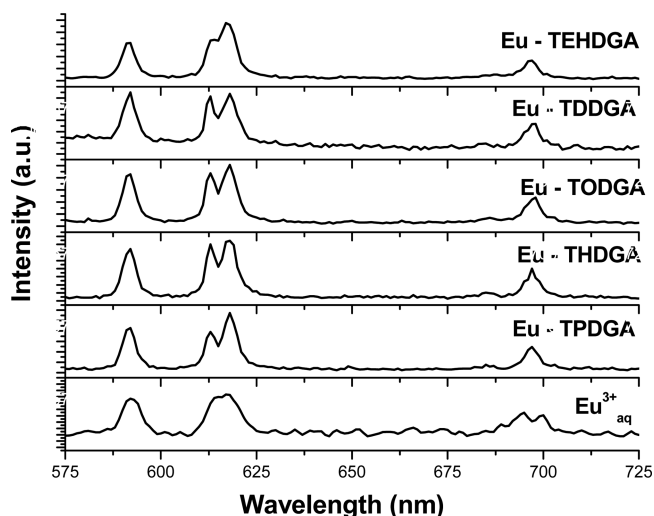


**Figure 5.** Emission profiles of  $\text{Eu}^{3+}_{\text{aq}}$  and different  $\text{Eu}^{3+}$ -DGA complexes in *n*-dodecane.

$^5\text{D}_0 \rightarrow ^7\text{F}_2$  transitions being hypersensitive electric-dipole transitions, the  $I(^5\text{D}_0 \rightarrow ^7\text{F}_2)$  is hypersensitive to the ligand field. In this study the asymmetry factor  $A$  follows the trend  $\text{Eu}^{3+}$ -TPDGA >  $\text{Eu}^{3+}$ -THDGA >  $\text{Eu}^{3+}$ -TODGA >  $\text{Eu}^{3+}$ -TPDGA (Table 8). This suggests that with increasing chain

**Table 8.** Characteristics of Different  $\text{Eu}^{3+}$ -DGA Complexes in *n*-Dodecane

complex	total lifetime ( $\tau$ ) ms	no. of species	$N(\text{H}_2\text{O})$	asymmetry factor ( $A$ )
Eu-TPDGA	2.17	1	0	2.027
Eu-THDGA	1.55	1	0	2.018
Eu-TODGA	2.15	1	0	1.919
Eu-TDDGA	1.94	1	0	1.605
Eu-T2EHDGA	1.54	1	0	2.358

length of the alkyl groups attached to the amidic nitrogens of the DGAs, the asymmetry around the metal ion decreases. For T2EHDGA, having a secondary alkyl group as the substituent, the asymmetry is expected to increase drastically. The asymmetry factor, lifetime, number of species, number of water molecules present in the inner coordination sphere of the metal ion, etc. for different  $\text{Eu}^{3+}$ -DGA complexes are summarized in Table 8. In all the cases the DGAs were found to form inner-sphere complexes with  $\text{Eu}^{3+}$  ion, i.e., there are no water molecules in the inner sphere of the  $\text{Eu}^{3+}$  ion. The nonradiative lifetimes ( $\tau_{\text{nr}}$ ) follow the trend  $\text{Eu}^{3+}$ -TODGA  $\sim$   $\text{Eu}^{3+}$ -TPDGA >  $\text{Eu}^{3+}$ -TDDGA >  $\text{Eu}^{3+}$ -T2EHDGA >  $\text{Eu}^{3+}$ -THDGA, while the quantum efficiency values ( $\eta$ ) follow the trend  $\text{Eu}^{3+}$ -TODGA  $\sim$   $\text{Eu}^{3+}$ -TPDGA >  $\text{Eu}^{3+}$ -TDDGA  $\sim$   $\text{Eu}^{3+}$ -T2EHDGA >  $\text{Eu}^{3+}$ -THDGA (Table 9). Wilden et al.,<sup>17</sup> have exhaustively studied the  $\text{Eu}^{3+}$  complexation with TODGA using TRFLS technique both in single phasic system in ethanol and in biphasic system in kerosene medium. They reported the formation of 1:1 and 1:3 complexes in ethanol medium, whereas in two phase extraction system in kerosene medium, similar to our observation the presence of only 1:3 complex was reported with the lifetime value of 2.46 ms. Similarly single extracted species in the two phase extraction of  $\text{Eu}^{3+}$  using *N,N'*-dimethyl-*N,N'*-dioctyl diglycolamides (DMDODGA) in

**Table 9.** Photophysical Properties of Different  $\text{Eu}$ -DGA Complexes Calculated from Luminescence Data

system	Eu-TPDGA	Eu-THDGA	Eu-TODGA	Eu-TDDGA	Eu-TEHDGA
radiative lifetime ( $\tau_r$ ) ms	5.76	5.61	5.78	6.20	5.20
nonradiative lifetime ( $\tau_{\text{nr}}$ ) ms	3.49	2.14	3.42	2.82	2.20
quantum efficiency ( $\eta$ )	0.38	0.28	0.37	0.31	0.30

octanol-kerosene mixture is also reported by Kou et al., from the TRFLS study with 1:3 metal to ligand stoichiometry.<sup>35</sup>

## CONCLUSIONS

We explored some of the aspects of the complexation of diglycolamides with varying alkyl chain length with lanthanide and actinide ions in different oxidation states. Two-phase solvent extraction studies showed that increasing the length of the alkyl group from *n*-pentyl to *n*-dodecyl in the DGAs adversely affects the extraction efficiency of the ligand. This was also corroborated from single-phase complexation studies in methanol medium using UV-vis spectrophotometric titrations, which indicated a decrease in the complexation constant values with  $\text{Nd}^{3+}$ . However, the complexation constant values increased going from TMDGA (Figure 1, R = Me) to TPDGA (Figure 1, R = *n*-pentyl). Similar observation of increasing complexation efficiency with increasing alkyl chain length from TMDGA to TPrDGA was also noticed in the literature, which could nicely be explained from the  $\Delta G$  values calculated with the help of DFT-based calculations showing more negative  $\Delta G$  value with increasing alkyl chain length from TMDGA to TBDGA. DFT studies also indicated the effect of branching on the steric hindrance in the  $\text{Nd}^{3+}$  complex, which ultimately results in increasing of the metal-ligand bond lengths and unfavorable  $\Delta G$  value for the  $\text{Nd}^{3+}$  complexation with branched alkyl DGA derivative, T2MPrDGA. Luminescence studies on the two phase extracted complex of  $\text{Eu}^{3+}$  for different DGA derivatives showed the absence of water molecules in the inner coordination sphere of the  $\text{Eu}^{3+}$  ion forming the  $\text{EuL}_3^{3+}$  type of extracted complex in *n*-dodecane medium as also reported in the literature. Further structural and EXAFS studies are required to address issues like the extraordinary high extraction efficiency toward trivalent actinides and lanthanides.

## ASSOCIATED CONTENT

### Supporting Information

The Supporting Information is available free of charge on the ACS Publications website at DOI: 10.1021/acs.jpcc.6b11222.

UV-vis titration spectra,  $^1\text{H}$  NMR spectra of La-complexes of DGAs, optimized geometries of  $\text{Nd}^{3+}$  complexes of DGAs, and luminescence decay profiles of different  $\text{Eu}^{3+}$ -DGA complexes (PDF)

## AUTHOR INFORMATION

### Corresponding Author

\*E-mail: mpatra@barc.gov.in; Fax: +91-22-25505151.

### ORCID

Sk. Musharaf Ali: 0000-0003-0457-0580

Prasanta K. Mohapatra: 0000-0002-0577-1811



## Notes

The authors declare no competing financial interest.

## ACKNOWLEDGMENTS

The authors thank Dr. P.K.Pujari, Head Radiochemistry Division, for his keen interest in this work. They also thank Dr. G.B. Dhekane of Thermax, Pune, for DGA samples.

## REFERENCES

- (1) Mathur, J. N.; Murali, M. S.; Nash, K. L. Actinide Partitioning-A Review. *Solvent Extr. Ion Exch.* **2001**, *19*, 357–390.
- (2) Nash, K. L. A Review of the Basic Chemistry and Recent Developments in Trivalent f-Elements Separations. *Solvent Extr. Ion Exch.* **1993**, *11*, 729–768.
- (3) Ansari, S. A.; Pathak, P.; Mohapatra, P. K.; Manchanda, V. K. Aqueous Partitioning of Minor Actinides by Different Processes. *Sep. Purif. Rev.* **2011**, *40*, 43–76.
- (4) Sasaki, Y.; Choppin, G. Extraction of Np(V) by *N,N'*-dimethyl-*N,N'*-dihexyl-3-oxapentanediamide. *Radiochim. Acta* **1998**, *80*, 85–88.
- (5) Ansari, S. A.; Pathak, P. N.; Husain, M.; Prasad, A. K.; Parmar, V. S.; Manchanda, V. K. Extraction of Actinides Using *N,N,N',N'*-Tetraoctyl Diglycolamide (TODGA): A Thermodynamic Study. *Radiochim. Acta* **2006**, *94*, 307–312.
- (6) Sasaki, Y.; Sugo, Y.; Tachimori, S.; Suzuki, S. The Novel Extractants, Diglycolamides, for the Extraction of Lanthanides and Actinides in HNO<sub>3</sub>-*n*-Dodecane System. *Solvent Extr. Ion Exch.* **2001**, *19*, 91–103.
- (7) Ansari, S. A.; Pathak, P.; Mohapatra, P. K.; Manchanda, V. K. Chemistry of Diglycolamides: Promising Extractants for Actinide Partitioning. *Chem. Rev.* **2012**, *112*, 1751–1772.
- (8) Brown, J.; McLachlan, F.; Sarsfield, M.; Taylor, R.; Modolo, G.; Wilden, A. Plutonium Loading of Prospective Grouped Actinide Extraction (GANEX) Solvent Systems based on Diglycolamide Extractants. *Solvent Extr. Ion Exch.* **2012**, *30*, 127–141.
- (9) Kou, F.; Yang, S.; Zhang, L.; Teat, S. J.; Tian, G. Complexation of Ho(III) with Tetraalkyl-Diglycolamide in Aqueous Solutions and a Solid State Compared in Organic Solutions of Solvent Extraction. *Inorg. Chem. Commun.* **2016**, *71*, 41–44.
- (10) Iqbal, M.; Huskens, J.; Verboom, W.; Sypula, M.; Modolo, G. Synthesis and Am/Eu Extraction of Novel TODGA Derivatives. *Supramol. Chem.* **2010**, *22*, 827–837.
- (11) Chapron, S.; Marie, C.; Arrachart, G.; Miguiditchian, M.; Pellet-Rostaing, S. New Insight into the Americium/Curium Separation by Solvent Extraction Using Diglycolamides. *Solvent Extr. Ion Exch.* **2015**, *33*, 236–248.
- (12) Kawasaki, T.; Okumura, S.; Sasaki, Y.; Ikeda, Y. Crystal Structures of Ln(III) (Ln = La, Pr, Nd, Sm, Eu, and Gd) Complexes with *N,N,N',N'*-Tetraethyldiglycolamide Associated with Homoleptic [Ln(NO<sub>3</sub>)<sub>6</sub>]<sup>3-</sup>. *Bull. Chem. Soc. Jpn.* **2014**, *87* (2), 294–300.
- (13) Sasaki, Y.; Suzuki, H.; Sugo, Y.; Kimura, T.; Choppin, G. R. New Water-soluble Organic Ligands for Actinide Cations Complexation. *Chem. Lett.* **2006**, *35*, 256–257.
- (14) Sasaki, Y.; Sugo, Y.; Morita, K.; Nash, K. L. The Effect of Alkyl Substituents on Actinide and Lanthanide Extraction by Diglycolamide Compounds. *Solvent Extr. Ion Exch.* **2015**, *33*, 625.
- (15) Sasaki, Y.; Sugo, Y.; Kitatsuji, Y.; Kirishima, A.; Kimura, T.; Choppin, G. R. Complexation and Back Extraction of Various Metals by Water-soluble Diglycolamide. *Anal. Sci.* **2007**, *23*, 727–731.
- (16) Tian, G.; Teat, S. J.; Rao, L. Structural and Thermodynamic Study of the Complexes of Nd(III) with *N,N,N',N'*-Tetramethyl-3-oxa-glutaramide and the Acid Analogues. *Inorg. Chem.* **2014**, *53*, 9477–9485.
- (17) Wilden, A.; Modolo, G.; Lange, S.; Sadowski, F.; Beele, B. B.; Skerencak-Frech, A.; Panak, P. J.; Iqbal, M.; Verboom, W.; Geist, A.; Bosbach, D. Modified Diglycolamides for the An(III) + Ln(III) Co-separation: Evaluation by Solvent Extraction and Time Resolved Laser Fluorescence Spectroscopy. *Solvent Extr. Ion Exch.* **2014**, *32*, 119–137.
- (18) Zhu, Z.-X.; Sasaki, Y.; Suzuki, H.; Suzuki, S.; Kimura, T. Cumulative Study on Solvent Extraction of Elements by *N,N,N',N'*-tetraoctyl-3-oxapentanediamide (TODGA) from Nitric Acid into *n*-Dodecane. *Anal. Chim. Acta* **2004**, *527* (527), 163–168.
- (19) Panja, S.; Mohapatra, P. K.; Tripathi, S. C.; Manchanda, V. K. Studies on Uranium(VI) Pertraction across a *N,N,N',N'*-Tetraoctyldiglycolamide (TODGA) Supported Liquid Membrane. *J. Membr. Sci.* **2009**, *337*, 274–281.
- (20) Tian, G.; Shuh, D. K.; Beavers, C. M.; Teat, S. J. A Structural and Spectrophotometric Study on the Complexation of Am(III) with TMOGA in Comparison with the Extracted Complex of DMDOGA. *Dalton Trans.* **2015**, *44*, 18469–18474.
- (21) Becke, A. D. Density-Functional Exchange-Energy Approximation with Correct Asymptotic Behavior. *Phys. Rev. A: At., Mol., Opt. Phys.* **1988**, *38*, 3098–3100.
- (22) Lee, C.; Yang, W.; Parr, R. G. Development of the Colle-Salvetti Correlation-Energy Formula into a Functional of the Electron Density. *Phys. Rev. B: Condens. Matter Mater. Phys.* **1988**, *37*, 785–789.
- (23) Becke, A. D. Density-Functional Thermochemistry. III. The Role of Exact Exchange. *J. Chem. Phys.* **1993**, *98*, 5648–5652.
- (24) TURBOMOLE; Quantum Chemistry Group at the University of Karlsruhe: Germany, 1988.
- (25) Ahlrichs, R.; Bär, M.; Häser, M.; Horn, H.; Kölmel, C. Electronic Structure Calculations on Workstation Computers: The Program System Turbomole. *Chem. Phys. Lett.* **1989**, *162*, 165–169.
- (26) Gorelsky, S. I. AOMix: Program for Molecular Orbital Analysis, Version 6.X; University of Ottawa, 2013; <http://www.sgchem.net>.
- (27) Gorelsky, S. I.; Lever, A. B. P. Electronic Structure and Spectra of Ruthenium Diimine Complexes by Density Functional Theory and INDO/S. Comparison of the Two Methods. *J. Organomet. Chem.* **2001**, *635*, 187–196.
- (28) Wei, M.; He, Q.; Feng, X.; Chen, J. Physical Properties of *N,N,N',N'*-Tetramethyl Diglycolamide and Thermodynamic Studies of its Complexation with Zirconium, Lanthanides and Actinides. *J. Radioanal. Nucl. Chem.* **2012**, *293*, 689–697.
- (29) Ansari, S. A.; Pathak, P. N.; Husain, M.; Prasad, A. K.; Parmar, V. S.; Manchanda, V. K. *N,N,N',N'*-Tetraoctyl diglycolamide (TODGA): A Promising Extractant for Actinide-Partitioning from High-Level Waste (HLW). *Solvent Extr. Ion Exch.* **2005**, *23*, 463–479.
- (30) Jensen, M. P.; Yaita, T.; Chiarizia, R. Reverse-Micelle Formation in the Partitioning of Trivalent f-Element Cations by Biphasic Systems Containing a Tetraalkyl Diglycolamide. *Langmuir* **2007**, *23*, 4765–4774.
- (31) Pathak, P. N.; Ansari, S. A.; Mohapatra, P. K.; Manchanda, V. K.; Patra, A. K.; Aswal, V. K. Role of Alkyl Chain Branching on Aggregation Behavior of Two Symmetrical Diglycolamides: Small Angle Neutron Scattering Studies. *J. Colloid Interface Sci.* **2013**, *393*, 347–351.
- (32) Pearson, R. G. Recent Advances in the Concept of Hard and Soft Acids and Bases. *J. Chem. Educ.* **1987**, *64*, 561–567.
- (33) Pearson, R. G. Hard and Soft Acids and Bases. *J. Am. Chem. Soc.* **1963**, *85*, 3533–3539.
- (34) Shannon, R. D. Revised Effective Ionic Radii and Systematic Studies of Interatomic Distances in Halides and Chalcogenides. *Acta Crystallogr., Sect. A: Cryst. Phys., Diffr., Theor. Gen. Crystallogr.* **1976**, *32*, 751–767.
- (35) Kou, F.; Yang, S.; Qian, H.; Zhang, L.; Beavers, C. M.; Teat, S. J.; Tian, G. A Fluorescence Study on the Complexation of Sm(III), Eu(III) and Tb(III) with Tetraalkyldiglycolamides (TRDGA) in Aqueous Solution, in Solid State, and in Solvent Extraction. *Dalton Trans.* **2016**, *45*, 18484–18493.
- (36) Charbonnel, M.-C.; Berthon, C.; Berthon, L.; Boubals, N.; Burdet, F.; Duchesne, M.-T.; Guilbaud, P.; Mabile, N.; Petit, S.; Zorz, N. Complexation of Ln(III) and Am(III) with the Hydrosoluble TEDGA: Speciation and Thermodynamics Studies. *Procedia Chem.* **2012**, *7*, 20–26.
- (37) Pathak, P. N.; Ansari, S. A.; Godbole, S. V.; Dhobale, A. R.; Manchanda, V. K. Interaction of Eu<sup>3+</sup> with *N,N,N',N'*-Tetraoctyl

Diglycolamide: A Time Resolved Luminescence Spectroscopy Study. *Spectrochim. Acta, Part A* **2009**, *73*, 348–352.

(38) Wang, C.-Z.; Lan, J.-H.; Wu, Q.-Y.; Zhao, Y.-L.; Wang, X.-K.; Chai, Z.-F.; Shi, W.-Q. Density Functional Theory Investigations of the Trivalent Lanthanide and Actinide Extraction Complexes with Diglycolamides. *Dalton Trans.* **2014**, *43*, 8713–8720.

(39) Narbutt, J.; Wodyński, A.; Pecul, M. The Selectivity of Diglycolamide (TODGA) and Bis-Triazine-Bipyridine (BTBP) Ligands in Actinide/Lanthanide Complexation and Solvent Extraction Separation - a Theoretical Approach. *Dalton Trans.* **2015**, *44*, 2657–2666.

(40) Ali, Sk. M.; Pahan, S.; Bhattacharyya, A.; Mohapatra, P. K. Complexation Thermodynamics of Diglycolamide with f-Elements: Solvent Extraction and Density Functional Theory Analysis. *Phys. Chem. Chem. Phys.* **2016**, *18*, 9816–9828.

(41) Kawasaki, T.; Okumura, S.; Sasaki, Y.; Ikeda, Y. Crystal structures of Ln(III) (Ln = La, Pr, Nd, Sm, Eu, and Gd) Complexes with N,N,N',N'-tetraethyldiglycolamide Associated with Homoleptic  $[\text{Ln}(\text{NO}_3)_6]^{3-}$ . *Bull. Chem. Soc. Jpn.* **2014**, *87*, 294–300.

(42) Trumm, M.; Schimmelpfennig, B.; Geist, A. Structure and Separation Quality of Various N- and O-donor Ligands from Quantum-Chemical Calculations. *Nukleonika* **2015**, *60*, 847–851.

(43) *Solvent Extraction: Principles and Practice*, 2nd ed.; Rydberg, J., Cox, M., Musicas, C., Choppin, G. R., Eds.; Marcel Dekker, Inc: New York, 1992; p 185.

(44) Horrocks, W. D.; Sudnick, D. R. Lanthanide Ion Probes of Structure in Biology. Laser-Induced Luminescence Decay Constants Provide a Direct Measure of the Number of Metal-Coordinated Water Molecules. *J. Am. Chem. Soc.* **1979**, *101*, 334–346.

(45) Zhang, P.; Kimura, T. Complexation of Eu(III) with Dibutyl Phosphate and Tributyl Phosphate. *Solvent Extr. Ion Exch.* **2006**, *24*, 149–163.

(46) Sengupta, A.; Godbole, S. V.; Mohapatra, P. K.; Iqbal, M.; Huskens, J.; Verboom, W. Judd-Ofelt Parameters of Diglycolamide-Functionalized Calix[4]arene  $\text{Eu}^{3+}$  Complexes in Room Temperature Ionic Liquid for Structural Analysis: Effects of Solvents and Ligand Stereochemistry. *J. Lumin.* **2014**, *148*, 174–180.

(47) Mohapatra, P. K.; Sengupta, A.; Iqbal, M.; Huskens, J.; Verboom, W. Highly Efficient Diglycolamide-Based Task-Specific Ionic Liquids: Synthesis, Unusual Extraction Behaviour, Irradiation, and Fluorescence Studies. *Chem. - Eur. J.* **2013**, *19*, 3230–3238.